Enhancing Sensitivity of a Single ZnO Micro-/Nanowire Photodetector by Piezo-phototronic Effect

Qing Yang,[†,‡] Xin Guo,[‡] Wenhui Wang,[†] Yan Zhang,[†] Sheng Xu,[†] Der Hsien Lien,[†] and Zhong Lin Wang*[,†]

[†]School of Material Science and Engineering, Georgia Institute of Technology, Atlanta, Georgia 30332 and [‡]State Key Laboratory of Modern Optical Instrumentation, Department of Optical Engineering, Zhejiang University, Hangzhou 310027, China

ABSTRACT We demonstrate the piezoelectric effect on the responsivity of a metal−semiconductor−metal ZnO micro-/nanowire photodetector. The responsivity of the photodetector is respectively enhanced by 530%, 190%, 9%, and 15% upon 4.1 pW, 120.0 pW, 4.1 nW, and 180.4 nW UV light illumination onto the wire by introducing a −0.36% compressive strain in the wire, which effectively tuned the Schottky barrier height at the contact by the produced local piezopotential. After a systematic study on the Schottky barrier height change with tuning of the strain and the excitation light intensity, an in-depth understanding is provided about the physical mechanism of the coupling of piezoelectric, optical, and semiconducting properties. Our results show that the piezo-phototronic effect can enhance the detection sensitivity more than 5-fold for pW levels of light detection.

KEYWORDS: ZnO nanowire · Schottky contact · piezopotential · photodetector · piezo-phototronic effect

ZnO nanowires (NWs) have attracted a great deal of interest because of their unique semiconducting, piezoelectric, biocompatible, and optoelectronic properties, which are fundamental for their application in electronics, optoelectronics, biology, environmental science, and energy.[1−3] In the past decade, a large variety of functional ZnO NW devices, such as field effect transistors,[2,4] optically pumped lasers,[5−7] chemical and biological sensors,[8,9] light emitting diodes,[10,11] solar cells,[12,13] photodetectors,[14−18] have been demonstrated. Recently, by utilizing the coupling of piezoelectric and semiconducting properties of ZnO, nangenerators,[19−21] piezoelectric field effect transistors,[22,23] and piezoelectric diodes[24,25] based on ZnO NWs have been the subject of extensive investigations, which are referred to as piezotronic devices. Furthermore, the coupling of optical, mechanical, and electrical properties of ZnO NWs provides new opportunities for fabricating functional devices,[3,26] aimed at improving the performance of optoelectronic devices[27] and providing an effective method to integrate optomechanical devices with microelectronic systems.[26] A new field of piezo-phototronics is being formed.

The core of the piezotronic and piezo-phototronic devices are to use the internal piezoelectric field formed inside ZnO at the interface with metal contact, as a result of purposely introduced strain, to tune the charge transport/separation process at the contact. Our recent work shows the possibility of optimizing the output of a photocell by pieozopotential.[27] The investigation on photoconducting responses at different bending strains of a ZnO NW shows that the photocurrent drops and the decay time decreases with the increase in bending of the NW.[28] Here we report that the responsivity of a ZnO wire metal−semiconductor−metal (MSM) photodetector for detection of sub-μW/cm^2 UV light could be increased dramatically by introducing strain. We investigate the dependence of the derived change in Schottky barrier height with strain on the excitation light intensity, which provides an in-depth understanding about the physical mechanism of the coupling of piezoelectric, optical, and semiconducting properties.

RESULTS AND DISCUSSION

Our device is a metal−semiconductor−metal structure (MSM). The contacts at the two ends of the semiconductor wire are two back-to-back Schottky contacts. The device was fabricated by bonding a ZnO micro-/nanowire laterally on a polystyrene (PS) substrate, which has a thickness much larger than the diameter of the ZnO micro-/nanowire (see Experimental Section for details). The experimental setup is shown schematically in Figure 1. The mechanical behavior of the device was dominated by the substrate by considering the relative size of the wire

*Address correspondence to zhong.wang@mse.gatech.edu.

Received for review September 5, 2010 and accepted September 22, 2010.

Published online Xxxxxxxxx 00, 0000
10.1021/nn1022878

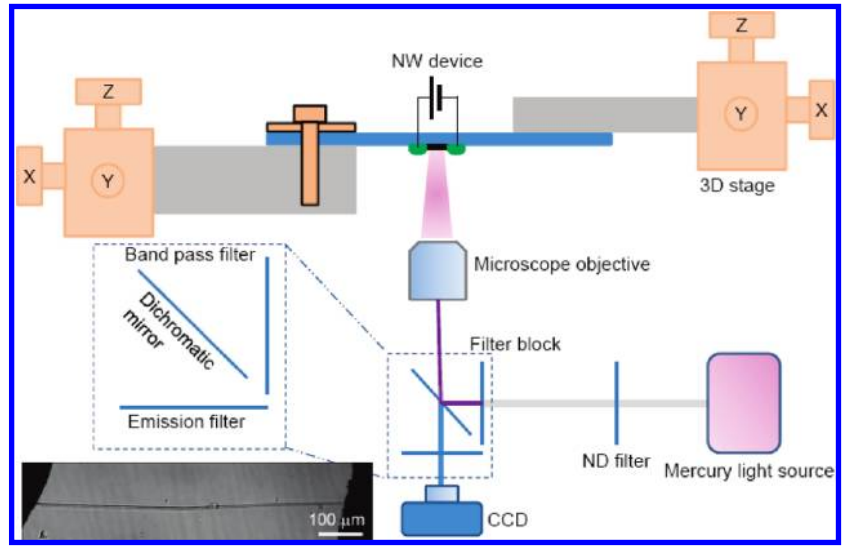

Figure 1. Schematic diagram of the measurement system to characterize the performance of the piezopotential tuned photodetector. An optical microscopy image of a ZnO wire device is shown.

and the substrate. The strain in the wire was mainly axial compressive or tensile strain depending on the bending direction of the PS substrate, and it was quantified by the maximum deflection of the free end of the substrate.[29] An optical image of the photodetector shown in Figure 1 indicated that a smooth ZnO wire was placed on the substrate with the two ends fixed. Monochromatic UV, blue, or green light was illuminated on the ZnO wire to test the performance of the device. The normalized spectrum of UV, blue, and green light is shown in Figure S1.

Before the electromechanical and optical measurements, we first measured the original $I-V$ characteristics of the device in the dark condition. Various $I-V$ characteristics were found in the experiments. In this study, we only focused on the devices that have symmetric Schottky contacts at the two ends of the ZnO wire and have very low dark current characteristics, which ensures the low noise and ultrasensitivity of the photodetector. The results of photocurrent measurements performed on a single ZnO wire device (Device #1) in standard ambient conditions are summarized in Figure 2. Figure 2a shows some typical $I-V$ characteristics of the ZnO wires in the dark and under UV illumination ($\lambda = 372$ nm) at various light intensities. The symmetric rectifying $I-V$ curves indicated that there were two back-to-back Schottky contacts at the two ends of the ZnO wire. As for the UV responsivity measurements in this paper, the bias was set at a fixed value of -5 V (reverse bias) for all of the measurements unless specifically indicated. The measured absolute current increased significantly with light illumination: the dark current was about 14 pA, and the current increased to 260 nA under 22 μW/cm^2 light illumination and further increased to 1.9 μA under 33 mW/cm^2 light illumination. The sensitivity defined as $(I_{light} - I_{dark})/I_{dark}$ was found to be 1.8×10^6% and 1.4×10^7% at 22 μW/cm^2 and 33 mW/cm^2 illumination, respectively. The sensitivity here is 1 or 2 orders of magnitude higher than that in a single Schottky contact device,[16,30] because of the very low dark current due to the depletion layer formed at the two Schottky contacts and oxygen-related hole trapping states at the ZnO wire surface. The spectral photoresponse of a ZnO wire photodetector showed a large UV-to-visible rejection ratio, which is defined as the sensitivity measured at UV divided by that at blue, and it was about 10^4 for the photodetector (Figure S1). The high spectral selectivity combined with high sensitivity suggests the possibility of using the ZnO wire photodetector as a 'visible-blind' UV photodetector for environmental, space-based, defense, and industrial applications. The photodetector was also measured with light on and off for many cycles with different light intensities, showing an excellent reversibility and stability with the decay time at about 1 s (Figure 2b). The relatively long reset time may be caused by the ultralong length of the wire which is used for easy and precise control of the strain in the wire.

The intensity dependences of photocurrents ($I_{ph} = |I_{light} - I_{dark}|$) are plotted in Figure 2c. The photocurrent increased linearly with the optical power and showed no saturation at high power levels, offering a large dynamic range from sub-μW/cm^2 to mW/cm^2. The total responsivity of the photodetector, $\mathcal{R}$, is defined as

$$\mathcal{R} = \frac{I_{ph}}{P_{ill}} = \frac{\eta_{ext} q}{h\upsilon} \cdot \Gamma_G \quad (1)$$

$$P_{ill} = I_{ill} \times d \times I \quad (2)$$

where $\mathcal{R}$ is the responsivity, I_{ph} the photocurrent, P_{ill} the illumination power on the photodetector, η_{ext} the external quantum efficiency, q the electronic charge, h Planck's constant, ν the frequency of the light, Γ_G the internal gain, I_{ill} the excitation power, d the diameter of

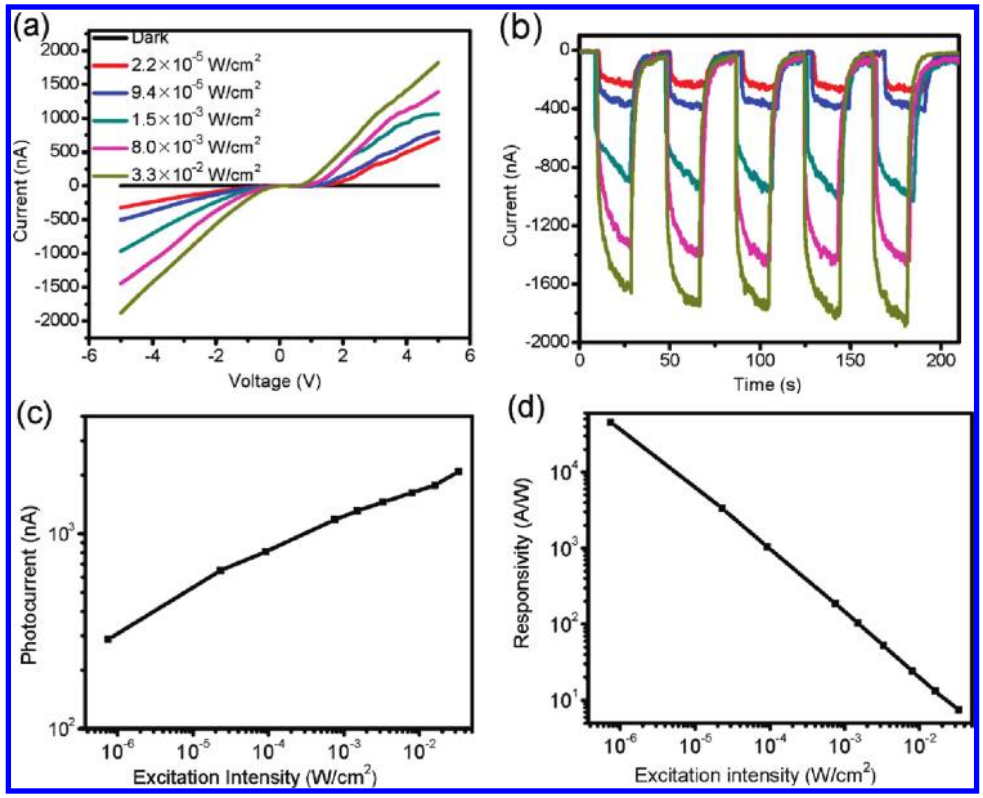

Figure 2. (a) *I*−*V* characteristics of a single ZnO wire photodetector (device #1) as a function of light intensity. (b) Repeatable response with different excitation light intensity, plotted in the same color code with (a). (c) Absolute photocurrent of a single ZnO wire device measured as a function of the excitation intensity. (d) Derived the photon responsivity relative to excitation intensity on the ZnO NW.

the ZnO wire, and *l* the spacing between two electrodes. Remarkably, the calculated responsivity of the device is super high, approximately 4.5×10^4 A W^{-1} at an intensity of 0.75 μW/cm^2 of UV light illumination. The internal gain can be estimated to be 1.5×10^5 by assuming $\eta_{ext} = 1$ for simplicity. The high internal gain and high responsivity is attributed to the oxygen-related hole trapping states[14] and the shrinking of the Schottky barrier upon illumination.[31] The decrease of the responsivity at relatively high light intensities is due to hole-trapping saturation and the Schottky barrier being transparent at high light intensity (Figure 2d).

We now use the MSM structure to illustrate the effects of the piezopotential on the performance of the photodetector (device #2). First, we investigated the effects of piezopotential on the dark current of the photodetector. Without strain, the dark current versus voltage curve of the device on a semilogarithmic scale was very flat (Figure 3 inset), even out to high bias, remaining <50 pA at a reverse bias of −20 V. We did not observe any evidence of breakdown due to the low level defects in the ZnO wire and good Schottky contact. *I*−*V* curves in the dark showed no change under different tensile and compressive strain (Figure 2a), which means that the piezopotential has a very small effect on the dark current. Then, we measured the *I*−*V* curve under variety of compressive and tensile strain upon UV illumination (Figures 2b and 2c). The absolute current at a negative bias increased step-by-step with application of a variable strain from 0.36% tensile to −0.36% compressing. Because the dark current did not change under strain, the sensitivity, responsivity, and detectivity of the photodetector increased under compressive strain. The responsivity of the photodetector under −0.36% compressive strain was enhanced by 530%, 190%, 9%, and 15% upon 0.75 μW/cm^2, 22 μW/cm^2, 0.75 mW/cm^2, and 33 mW/cm^2 illumination, respectively. The corresponding light power illuminated onto the ZnO wire was about 4.1 pW, 120.0 pW, 4.1 nW, and 180.4 nW, respectively. Figure 2d shows the absolute photocurrent relative to excitation intensity under different strains with a natural logarithmic scale. It can be seen that the photocurrent is largely enhanced for pW level light detection by using the piezoelectric effect. And it is pointed out that the effect of strain is much larger for weak light detection than for strong light detection.

In our experiments, some of the devices show opposite change when applying the same strain. As shown in Figures S2 and S3 (device #1), the absolute current decreased step-by-step with application of a variable strain from 0.26% tensile to −0.26% compressing. Tensile strain improved the responsivity of the photodetector. This phenomenon is attributed to the switching in signs of the piezoptential, which depends on the orientation of the *c* axis of the ZnO wire. We have 50%

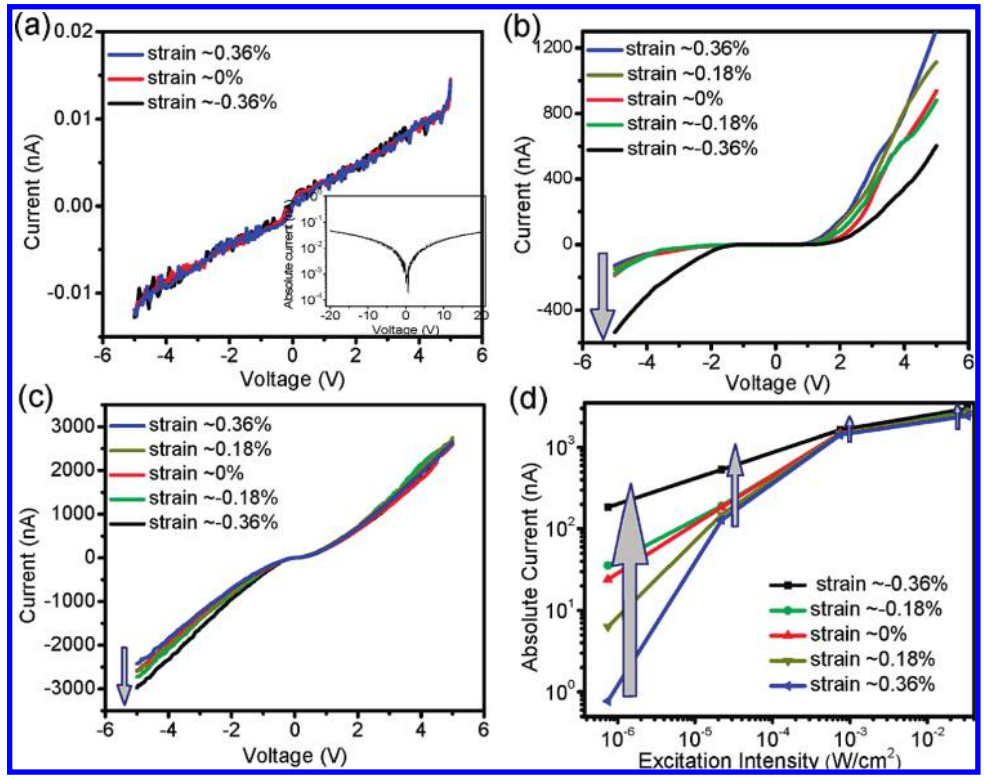

Figure 3. (a) Typical dark *I*−*V* characteristics of a ZnO wire device (device #2) under different strain. (b) *I*−*V* curves of the device under different strain with excitation light intensity of 2.2 × 10^{-5} W/cm²; the power illuminated on the nanowire was 120 pW, responsivity was increased by 190% under −0.36% compressive strain. (c) *I*−*V* curves of the device under different strain with excitation light intensity of 3.3 × 10^{-2} W/cm²; the power illuminated on the nanowire was 180.4 nW, responsivity was increased by 15% under compressive −0.36% strain. (d) Absolute photocurrent relative to excitation intensity of device #2 under different strain.

chance in experiments to have the ZnO wire oriented along the *c* or −*c* direction (the axial direction of the wires).

Our device can be considered as a single ZnO wire sandwiched between two back-to-back Schottky diodes, as shown in Figure 5. In our case, when a relatively large negative voltage was applied, the voltage drop occurred mainly at the reversely biased Schottky barrier ϕ_d at the drain side, which is denoted as $V_d \approx V$. Under reverse bias and under dark conditions, thermionic emission with barrier lowering is usually the dominant current transport mechanism at a Schottky barrier, which can be described by the thermionic-emission-diffusion theory (for $V \gg 3kT/q \approx 77$ mV) as[32]

$$I_{TED}^{dark} = SA^{**}T^2\exp\left[-\frac{1}{kT}\cdot(q\varphi_d^{dark})\right] \times \exp\left(\frac{1}{kT}\cdot\xi^{1/4}\right) \quad (3)$$

$$\xi = q^7 N_D (V + V_{bi} - kT/q)/8\pi^2\varepsilon_s^3 \quad (4)$$

$$V_{bi} = \varphi_d^{dark} - (E_C - E_f) \quad (5)$$

in which *S* is the area of the Schottky contact, A^{**} the effective Richardson constant, *T* the temperature, *q* the unit electronic charge, *k* the Boltzmann constant, N_D the donor impurity density, *V* the applied voltage, V_{bi} the built-in potential, and ε_s the permittivity of ZnO.

The effect of photoillumination on semiconductor thermionic emission is to lower the energy barrier by the difference between the quasi-Fermi level with photoexcitation and the Fermi level without photoexcitation[33] and to reduce the width of the depletion layer by photon generated holes trapped in the depletion layer (Figure 5c). The current transport mechanism with illumination can be described as

$$I_{TED}^{ill} = SA^{**}T^2\exp\left\{-\frac{1}{kT}\cdot[q\varphi_d^{dark} - (E_{FN} - E_f)]\right\} \times \exp\left(\frac{1}{kT}\cdot\xi^{1/4}\right) = SA^{**}T^2\exp\left[-\frac{1}{kT}\cdot(q\varphi_d^{ill})\right] \times \exp\left(\frac{1}{kT}\cdot\xi^{1/4}\right) \quad (6)$$

where E_{FN} is the quasi Fermi level with illumination.

The ln[*I*/(1 nA)] − *V* curve shown in Figure 4a qualitatively indicates that the variation of ln[*I*/(1 nA)] can be described by the power law of $V^{1/4}$ for the reversely biased Schottky barrier. However, the slope and extended zero voltage point for the fitting data with light illumination are larger than those in the dark. According to eqs 3 and 6, the difference may be attributed to an effective lowering of the Schottky barrier and the change of N_D due to the holes trapped in the depletion region.

By assuming *S*, A^{**}, *T*, and N_D are independent of strain at small deformation, the change in Schottky bar-

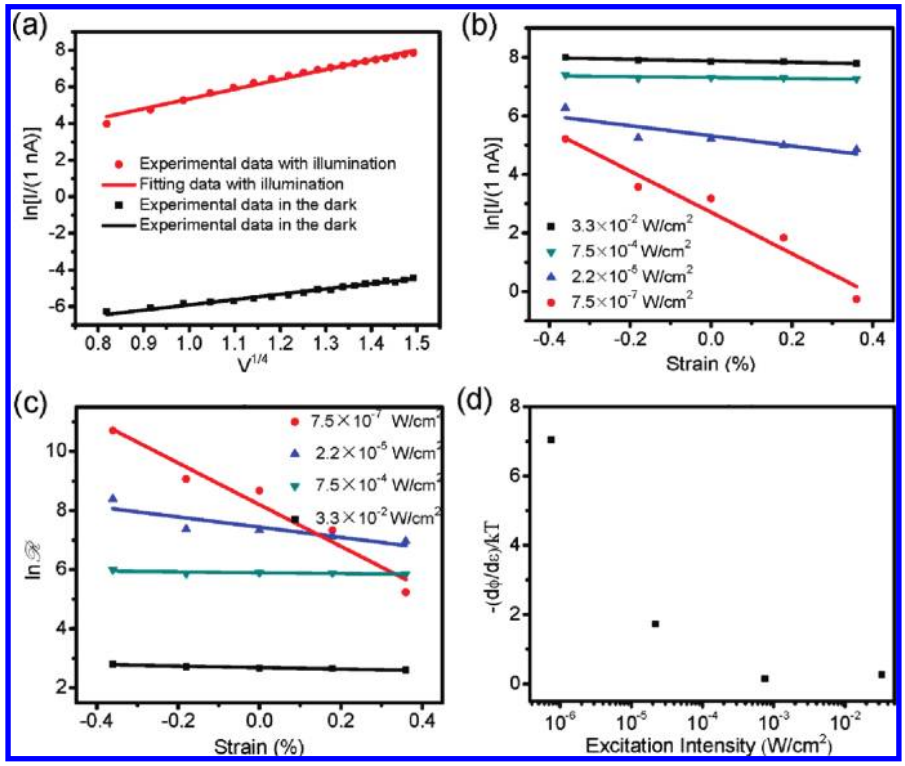

Figure 4. (a) Plot of ln[*I*/(1 nA)] as a function of $V^{1/4}$, by using the data from Figure 3a and c for the case of without strain. The red circles and line represent the experimental data and fitting curve with 3.3 × 10^{-2} W/cm^2 light illumination. The black squares and line represent the experimental data and fitting curve in the dark condition. (b) Plot of ln[*I*/(1 nA)] as a function of strain under different excitation light intensity. (c) Responsivity (units A/W) as a function of strain under different excitation light intensity on a natural logarithmic scale. (d) The derived change of Schottky barrier height with strain as a function excitation light intensity.

rier height (SBH) with strain upon illumination can be determined by

$$\ln\left[\frac{I(\varepsilon_{xx})}{I(0)}\right] = -\frac{\Delta\varphi_d^{ill}}{kT} \quad (7)$$

where $I(\varepsilon_{xx})$ and $I(0)$ are the current measured through the ZnO wire at a fixed bias with and without strain applied, respectively. Figure 4b shows the ln[*I*/(1 nA)] as a function of strain with different excitation light intensities on a natural logarithmic scale. The results indicate that the change of SBH has an approximately linear relationship with strain. Furthermore, the slope of the change of SBH varies with the excitation light intensity. It means that the derived change in barrier height with strain depends on the excitation light intensity and the SBH changes faster at low light intensity than that at high light intensity (Figure 4d). The change in the total responsivity of the photodetector with strain is similar to the change in current; the difference is that the current increases with increasing light intensity but the responsivity decreases.

It is known that the change in the Schottky barrier height under strain is a combined effect from both strain induced band structure change (e.g., piezoresistance) and piezoelectric polarization.[24,29,34,35] The contributions from the band structure effect to SBH in source and drain contacts are denoted as $\Delta\phi_{d\text{-}bs}$ and $\Delta\phi_{s\text{-}bs}$, respectively. Assuming the axial strain is uniform in the ZnO wire along its entire length, $\Delta\phi_{d\text{-}bs} = \Delta\phi_{s\text{-}bs}$ if the two contacts are identical. This is the piezoresistance effect, which is symmetric and has equal effects regardless of the polarity of the voltage. The asymmetric change of the *I*−*V* curve at negative and positive bias in our case is dominated by the piezoelectric effect rather than the piezoresistance effect. The effect of piezopotential to the SBH can be qualitatively described as follows. For a constant strain of ε_{xx} along the length of the wire, an axial polarization $P_x = \varepsilon_{xx}e_{33}$ occurs, where e_{33} is the piezoelectric tensor. A potential drop of approximately $V_p^+ - V_p^- = \varepsilon_{xx}Le_{33}$ is along the length of the wire, where *L* is the length of the wire. Therefore, modulations to the SBH at the source and drain sides are of the same magnitude but opposite in sign ($V_p^+ = -V_p^-$), which are denoted by $\Delta\phi_{d\text{-}pz}$ and $\Delta\phi_{s\text{-}pz}$ ($\Delta\phi_{d\text{-}pz} = -\Delta\phi_{s\text{-}pz}$).

In the experiments, we fixed the light intensity and bent the substrate step-by-step; thus strain was introduced into the device step-by-step. Depending on the deformation direction, the sign of the strain was changed from positive to negative or vice versa. Meanwhile, the corresponding piezopotential distribution in the wire was also adjusted step-by-step, which changed the effective heights of the two Schottky barriers and thus the photocurrent and responsivity of the device. Figure 5a shows a numerically calculated piezopoten-

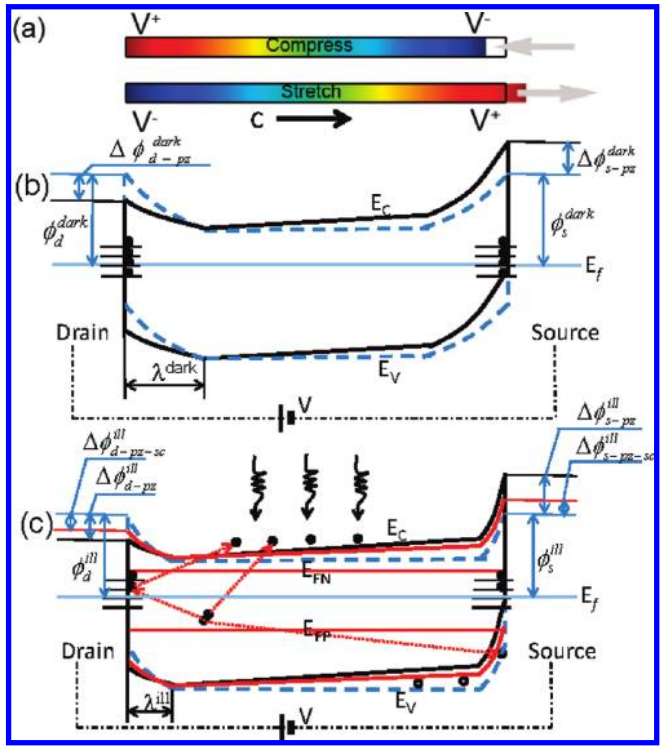

Figure 5. Schematic energy band diagram illustration for tuning the barrier height by piezopotential. (a) Simulation of the piezopotential distribution in the wire under compressive and tensile strain; the diameter and length used for calculation is about 1 and 20 μm, respectively. The pressure on *c*-plane is about ±1 MPa. (b) Barrier height tuned by piezopotential under compressive strain in the dark. (c) Barrier height tuned by piezopotential under compressive strain with light illumination

tial distribution in the wire using the finite element method without considering the natural doping. If the nanowire is positioned along the *c*-axis direction from the drain to source side, a positive potential drop will be induced along the length of the wire under compressive strain. Therefore the SBH at the drain contacts were decreased with increasing compressive strain; simultaneously the photocurrent and responsivity were increased under compressive strain.

The effect of piezopotential decreases with increasing light intensity (Figure 4d), which may be caused by the screening effect of the newly generated charge carriers to the piezopotential. When the ZnO wire is under high light intensity, large amount of free electrons and holes are generated. They will accumulate and cause the piezoelectrical potential to be partially screened, and $\Delta\phi_{d\text{-}pz}$ will be decreased to $\Delta\phi_{d\text{-}pz\text{-}sc}$ (Figure 5c).

It is interesting that the piezoelectric effect on the *I*−*V* curve in the dark is not obvious either (Figure 3a). In the dark, the surface of the ZnO wire is depleted by absorbed oxygen molecules and the dark current is very low (about 14 pA at −5 V applied bias). In this case, the device can be considered as an insulator wire sandwiched between two back-to-back Schottky diodes, and the current is controlled by the bulk of the sample, not by the Schottky contact. Thus although piezopotential tunes the SBH, it cannot have a dominant effect on the dark current. Therefore, piezopotential dramatically increases the responsivity for pW level light detection while maintaining the low dark current characteristics of the devices, which is very useful for applications.

CONCLUSIONS

In summary, we have demonstrated a piezopotential tuned low dark-current ultrasensitive ZnO wire photodetector. The device maintains low dark current characteristics while increasing the responsivity dramatically for pW level light detection by piezopotential. The derived change in barrier height with strain depends on excitation light intensity; the SBH changes faster at low light intensity than that at high light intensity. The physical mechanism is explained by considering both the piezopotential effect and photon generated free charge screening effect. Three-way coupling of semiconducting, photonic and piezoelectric properties of semiconductor nanowires will allow tuning and control of the electro-optical process by strain induced piezopotential, which is the piezo-phototronic effect, and it will also lead to further integration between piezoelectric devices with microelectronic and optomechanical systems.

EXPERIMENTAL SECTION

The ZnO micro/nanowires used in our study were synthesized by a high-temperature thermal evaporation process.[36] The detailed device fabrication process was introduced elsewhere.[24,29] Briefly, a single ZnO wire was bonded on a PS substrate (typical length of ~7 cm, width of ~15 mm, and thickness of 0.5 mm) by silver pastes. A very thin layer of polydimethylsiloxane (PDMS) was used to package the device, which kept the device mechanically robust under repeated manipulation and prevented the semiconductor wire from contamination or corrosion. A 3D stage with movement resolution of 1 μm was used to bend the free end of the device to produce a compressive and tensile strain. Another 3D stage was used to fix the sample under a microscope and to keep the device in focus during the substrate bending process.

A Nikon Eclipse Ti inverted microscope system was used to monitor the sample and excite the photodetector. A Nikon Intensilight C-HGFIE lamp with a remote controller was used as the excitation source. Monochromatic UV (centered at 372 nm), blue (centered at 486 nm), or green light (centered at 548 nm) was illuminated on the ZnO wire to test the performance of the device, which was focused by a 10× microscope objective with a 17.5 mm work distance. Monochromatic light was obtained by a filter block between the source and microscope objective (Figure 1). There were three sets of filter blocks which were used to obtain monochromatic UV, blue, and green light. The optical power density impinging on the nanowire photodetector was varied by means of neutral density filters. The illumination density was determined by a thermopile power meter (Newport 818P-001-12). *I*−*V* measurement was obtained by applying an external bias to the wire and recorded using a Keithley 487 picoammeter/voltage source in conjunction with a GPIB controller (National Instruments GPIB-USB-HS, NI 488.2). In order to

compare and analyze the results, time dependent photocurrent, light intensity dependent photocurrent, and photocurrent used for analyzing responsivity and strain effects were measured at a fixed applied bias of −5 V.

Acknowledgment. Research was supported by BES DOE (DE-FG02-07ER46394), Airforce, NSF (DMS0706436, CMMI0403671), and NSFC (60706020). Thanks are extended to Youfan Hu, Rusen Yang, Hao Fang, and Zetang Li for technical assistance.

Supporting Information Available: Experimental details. This material is available free of charge via the Internet at http://pubs.acs.org.

REFERENCES AND NOTES

1. Wang, Z. L. ZnO Nanowire and Nanobelt Platform for Nanotechnology. *Mater. Sci. Eng. R* **2009**, *64*, 33–71.
2. Heo, Y. W.; Norton, D. P.; Tien, L. C.; Kwon, Y. S.; Kang, B. S.; Ren, F.; Pearton, S. J.; LaRoche, J. R. ZnO Nanowire Growth and Devices. *Mater. Sci. Eng. R* **2004**, *47*, 1–47.
3. Wang, Z. L.; Yang, R.; Zhou, J.; Qin, Y.; Xu, C.; Hu, Y.; Xu, S. Lateral Nanowire/Nanobelt Based Nanogenerators, Piezotronics and Piezo-Phototronics. *Mater. Sci. Eng. R* 2010, doi:10.1016/j.mser.2010.06.015.
4. Goldberger, J.; Sirbuly, D. J.; Law, M.; Yang, P. ZnO Nanowire Transistors. *J. Phys. Chem. B* **2005**, *109*, 9–14.
5. Zimmler, M. A.; Bao, J. M.; Capasso, F.; Muller, S.; Ronning, C. Laser Action in Nanowires: Observation of the Transition from Amplified Spontaneous Emission to Laser Oscillation. *Appl. Phys. Lett.* **2008**, *93*, 051101.
6. Huang, M. H.; Mao, S.; Feick, H.; Yan, H. Q.; Wu, Y. Y.; Kind, H.; Weber, E.; Russo, R.; Yang, P. D. Room-Temperature Ultraviolet Nanowire Nanolasers. *Science* **2001**, *292*, 1897–1899.
7. Yang, Q.; Jiang, X.; Guo, X.; Chen, Y.; Tong, L. Hybrid Structure Laser Based on Semiconductor Nanowires and a Silica Microfiber Knot Cavity. *Appl. Phys. Lett.* **2009**, *94*, 101108.
8. Wan, Q.; Li, Q. H.; Chen, Y. J.; Wang, T. H.; He, X. L.; Li, J. P.; Lin, C. L. Fabrication and Ethanol Sensing Characteristics of ZnO Nanowire Gas Sensors. *Appl. Phys. Lett.* **2004**, *84*, 3654–3656.
9. Choi, A.; Kim, K.; Jung, H. I.; Lee, S. Y. ZnO Nanowire Biosensors for Detection of Biomelecular Interactions in Enhancement Mode. *Sens. Actuators, B* **2010**, *148*, 577–582.
10. Bao, J. M.; Zimmler, M. A.; Capasso, F.; Wang, X. W.; Ren, Z. F. Broadband ZnO Single-Nanowire Light-Emitting Diode. *Nano Lett.* **2006**, *6*, 1719–1722.
11. Willander, M.; Nur, O.; Zhao, Q. X.; Yang, L. L.; Lorenz, M.; Cao, B. Q.; Perez, J. Z.; Czekalla, C.; Zimmermann, G.; Grundmann, M.; et al. Zinc Oxide Nanorod Based Photonic Devices: Recent Progress in Growth, Light Emitting Diodes and Lasers. *Nanotechnology* **2009**, *20*, 332001.
12. Law, M.; Greene, L. E.; Johnson, J. C.; Saykally, R.; Yang, P. D. Nanowire Dye-Sensitized Solar Cells. *Nat. Mater.* **2005**, *4*, 455–459.
13. Weintraub, B.; Wei, Y.; Wang, Z. L. Optical Fiber/Nanowire Hybrid Structures for Efficient Three-Dimensional Dye-Sensitized Solar Cells. *Angew. Chem., Int. Ed.* **2009**, *48*, 1–6.
14. Soci, C.; Zhang, A.; Xiang, B.; Dayeh, S. A.; Aplin, D. P. R.; Park, J.; Bao, X. Y.; Lo, Y. H.; Wang, D. ZnO Nanowire UV Photodetectors with High Internal Gain. *Nano Lett.* **2007**, *7*, 1003–1009.
15. Aga, R. S.; Jowhar, D.; Ueda, A.; Pan, Z.; Collins, W. E.; Mu, R.; Singer, K. D.; Shen, J. Enhanced Photoresponse in ZnO Nanowires Decorated with CdTe Quantum Dot. *Appl. Phys. Lett.* **2007**, *91*, 232108.
16. Zhou, J.; Gu, Y. D.; Hu, Y. F.; Mai, W. J.; Yeh, P. H.; Bao, G.; Sood, A. K.; Polla, D. L.; Wang, Z. L. Gigantic Enhancement in Response and Reset Time of ZnO UV Nanosensor by Utilizing Schottky Contact and Surface Functionalization. *Appl. Phys. Lett.* **2009**, *94*, 191103.
17. Kim, W.; Chu, K. S. ZnO Nanowire Field-Effect Transistor as a UV Photodetector; Optimization for Maximum Sensitivity. *Phys. Status Solidi A* **2009**, *206*, 179–182.
18. Chen, M. W.; Chen, C. Y.; Lien, D. H.; Ding, Y.; He, J. H. Photoconductive Enhancement of Single ZnO Nanowire through Localized Schottky Effects. *Opt. Express* **2010**, *18*, 14836–14841.
19. Wang, Z. L.; Song, J. H. Piezoelectric Nanogenerators Based on Zinc Oxide Nanowire Arrays. *Science* **2006**, *312*, 242–246.
20. Wang, X. D.; Song, J. H.; Liu, J.; Wang, Z. L. Direct-Current Nanogenerator Driven by Ultrasonic Waves. *Science* **2007**, *316*, 102–105.
21. Cha, S. N.; Seo, J. S.; Kim, S. M.; Kim, H. J.; Park, Y. J.; Kim, S. W.; Kim, J. M. Sound-Driven Piezoelectric Nanowire-Based Nanogenerators. *Adv. Mater.* 2010, DOI:10.1002/adma.201001169.
22. Wang, X. D.; Zhou, J.; Song, J. H.; Liu, J.; Xu, N. S.; Wang, Z. L. Piezoelectric Field Effect Transistor and Nanoforce Sensor Based on a Single ZnO Nanowire. *Nano Lett.* **2006**, *6*, 2768–2772.
23. Fei, P.; Yeh, P. H.; Zhou, J.; Xu, S.; Gao, Y. F.; Song, J. H.; Gu, Y. D.; Huang, Y. Y.; Wang, Z. L. Piezoelectric Potential Gated Field-Effect Transistor Based on a Free-Standing ZnO Wire. *Nano Lett.* **2009**, *9*, 3435–3439.
24. Zhou, J.; Fei, P.; Gu, Y. D.; Mai, W. J.; Gao, Y. F.; Yang, R.; Bao, G.; Wang, Z. L. Piezoelectric-Potential-Controlled Polarity-Reversible Schottky Diodes and Switches of ZnO Wires. *Nano Lett.* **2008**, *8*, 3973–3977.
25. Yang, Y.; Qi, J. J.; Liao, Q. L.; Li, H. F.; Wang, Y. S.; Tang, L. D.; Zhang, Y. High-Performance Piezoelectric Gate Diode of a Single Polar-Surface Dominated ZnO Nanobelt. *Nanotechnology* **2009**, *20*, 125201.
26. Eichenfield, M.; Chan, J.; Camacho, R. M.; Vahala, K. J.; Painter, O. Optomechanical Crystals. *Nature* **2009**, *462*, 78–82.
27. Hu, Y. F.; Zhang, Y.; Chang, Y. L.; Snyder, R. L.; Wang, Z. L. Optimizing the Power Output of a ZnO Photocell by Piezopotential. *ACS Nano* **2010**, *4*, 4220–4224.
28. Gao, P.; Wang, Z. Z.; Liu, K. H.; Xu, Z.; Wang, W. L.; Bai, X. D.; Wang, E. G. Photoconducting Response on Bending of Individual ZnO Nanowires. *J. Mater. Chem.* **2009**, *19*, 1002–1005.
29. Zhou, J.; Gu, Y. D.; Fei, P.; Mai, W. J.; Gao, Y. F.; Yang, R. S.; Bao, G.; Wang, Z. L. Flexible Piezotronic Strain Sensor. *Nano Lett.* **2008**, *8*, 3035–3040.
30. Wei, T. Y.; Huang, C. T.; Hansen, B. J.; Lin, Y. F.; Chen, L. J.; Lu, S. Y.; Wang, Z. L. Large Enhancement in Photon Detection Sensitivity Via Schottky-Gated CdS Nanowire Nanosensors. *Appl. Phys. Lett.* **2010**, *96*, 013508.
31. Mehta, R. R.; Sharma, B. S. Photoconductive Gain Greater Than Unity in CdSe Films with Schottky Barriers at Contacts. *J. Appl. Phys.* **1973**, *44*, 325–328.
32. Sze, S. M. *Physics of Semiconductor Devices*; Wiley: New York, 1981.
33. Schwede, J. W.; Bargatin, I.; Riley, D. C.; Hardinm, B. E.; Rosenthal, S. J.; Sun, Y.; Schmitt, F.; Pianetta, P.; Howe, R. T.; Shen, Z.; Melosh, N. A. Photon-Enhanced Thermionic Emission for Solar Concentrator Systems. *Nat. Mater.* **2010**, *9*, 762–767.
34. Ki-Woong Chung, Z. W.; Costa, J. C.; Williamson, F.; Ruden, P. P.; Nathan, M. I. Barrier Height Change in GaAs Schottky Diodes Induced by Piezoelectric Effect. *Appl. Phys. Lett.* **1991**, *59*, 1191–1193.
35. Shan, W.; Li, M. F.; Yu, P. Y.; Hansen, W. L.; Walukiewicz, W. Pressure-Dependence of Schottky-Barrier Height at the Pt/GaAs Interface. *Appl. Phys. Lett.* **1988**, *53*, 974–976.
36. Pan, Z. W.; Dai, Z. R.; Wang, Z. L. Nanobelts of Semiconducting Oxides. *Science* **2001**, *291*, 1947–1949.